TGF-β receptor-specific NanoBRET target engagement in living cells for high-throughput kinase inhibitor screens

Wits, M.; Haarmans, N.; Sanchez Duffhues, G.; Goumans, M.J.

SLAS Discovery 29 (2024) 100196

Contents lists available at ScienceDirect

SLAS Discovery

journal homepage: www.elsevier.com/locate/slasd

TGF-β receptor-specific NanoBRET Target Engagement in living cells for high-throughput kinase inhibitor screens

Marius Wits [a], Nicole Haarmans [a], Gonzalo Sanchez-Duffhues [a,b,1,*], Marie-José Goumans [a,1,*]

[a] Department of Cell and Chemical Biology, Leiden University Medical Center, Einthovenweg 20, 2333 ZC, Leiden, the Netherlands
[b] Nanomaterials and Nanotechnology Research Center (CINN), Spanish National Research Council (CSIC), Health Research Institute of Asturias (ISPA), 33011 Oviedo, Asturias, Spain

ARTICLE INFO

Keywords:
BMP
Drug development
Rare disease
Cancer
Angiogenesis

ABSTRACT

Targeting transforming growth factor-β (TGF-β) receptors is a promising pharmacological approach to normalize aberrant signaling in genetic and non-genetic TGF-β associated diseases including fibrosis, cancer, cardiovascular and musculoskeletal disorders. To identify novel TGF-β receptor kinase inhibitors, methods like in vitro kinase assays, western blot or transcriptional reporter assays are often used for screening purposes. While these methods may have certain advantages, the lack of integration of key features such as receptor specificity, high-throughput capability, and cellular context resemblance remains a major disadvantage. This deficiency could ultimately hinder the translation of study outcomes into later (clinical) stages of drug development. In this study, we introduce an adjusted and optimized live cell NanoBRET Target Engagement (TE)-based method to identify TGF-β receptor specific kinase inhibitors. This comprehensive toolkit contains various TGF-β type I and type II receptors, with corresponding nanoBRET tracers, and disease-related cell lines, including novel non-commercially available materials. The nanoBRET capacity and kinase inhibitory window can be significantly enhanced for functional measurements when stable expression cell lines and substantially low tracer concentrations are used. In addition, this system can be tailored to study TGF-β associated genetic disorders and possibly be used to screen for disease-specific therapeutics. Therefore, the use of this optimized, live cell, antibody-independent nanoBRET Target Engagement assay is highly encouraged for future high-throughput compound screens targeting TGF-β/BMP receptors.

1. Introduction

1.1. Introducing TGF-β signaling in health and disease

Transforming growth factor-β (TGF-β) signal transduction is crucial for proper tissue development and homeostasis [1]. This broad signaling pathway consists of more than 30 different ligands, including TGF-β1-3, Activins, Bone morphogenetic proteins (BMPs) and Growth differentiation factors (GDFs) [2–4]. To exert their biological actions, TGF-β superfamily ligands bind their respective tetrameric serine/threonine receptor complexes, formed by two type I (i.e. Activin receptor-like kinase (ALK)1-7) and two type II receptors (i.e. Activin A receptor type II A (ACVR2A), ACVR2B, TGF-β Receptor 2 (TGFβR2), BMPR2, or Anti--Müllerian Hormone Receptor 2 (AMHR2)) (Fig. 1A) [4,5]. TGF-β superfamily ligands show different affinities for their membrane receptors. As such, high-affinity receptors are different for Activins (ALK4 and ALK7), TGF-β_{1-3} (ALK5), and BMPs (ALK1, ALK2, ALK3 or ALK6) [6,7]. In addition, low-affinity complexes are formed too, and the relative ligand concentration and cellular receptor expression levels are therefore important factors to consider. In this regard, soluble antagonists like Follistatin can reduce ligand availability [8]. Furthermore, co-receptors (e.g. Betaglycan or Endoglin) can enhance or reduce the formation of receptor complexes [9]. Downstream mediators of the TGF-β signaling pathway are the small mothers against decapentaplegic 1–5 and 8 (SMAD1/2/3/5/8). In a canonical setting, receptor-regulated SMADs (R-SMADs) SMAD2 and -3 are phosphorylated by ALK4, -5 or -7; and SMAD1, -5, and -8 are phosphorylated by the BMP type I receptors ALK1, -2, -3, or -6 [10]. Subsequently, these activated R-SMADs form a trimer with Co-SMAD4 and harbor its transcriptional activity driving important cellular processes including proliferation and differentiation.

* Corresponding authors at: Department of Cell and Chemical Biology, Leiden University Medical Center, Einthovenweg 20, 2333 ZC Leiden, the Netherlands.
E-mail addresses: g.s.duffhues@cinn.es (G. Sanchez-Duffhues), m.j.t.h.goumans@lumc.nl (M.-J. Goumans).
[1] These authors contributed equally.

https://doi.org/10.1016/j.slasd.2024.100196
Received 27 June 2024; Received in revised form 7 November 2024; Accepted 11 November 2024
Available online 12 November 2024

Negative feedback mechanisms are in place, where for instance SMAD6 and -7 are canonical intracellular inhibitors, directly acting as R-SMAD decoy and/or recruiting ubiquitin-dependent degradation of R-SMADs and TGF-β receptors [11,12]. If disturbed, disbalanced TGF-β signaling can result in a multitude of genetic and non-genetic disorders such as fibrosis [13,14], cancer [14,15], musculoskeletal disorders [16] and cardiovascular diseases [14,17].

Targeting TGF-β receptors by small molecule kinase inhibitors is a well-acknowledged and promising pharmacological approach to treat many of these TGF-β associated disorders [18,19]. For example, in the rare musculoskeletal disorder Fibrodysplasia ossificans progressiva (FOP), the gain-of-function mutation p.R206H in ALK2 causes heterotopic bone formation and kinase inhibitors targeting ALK2 have shown to be highly effective in pre-clinical models [20,21]. Also, in the cardiovascular disease Pulmonary arterial hypertension (PAH) a disbalance in SMAD2/3 over SMAD1/5/8 signaling as a result of e.g. BMPR2 loss-of-function mutations, causes pulmonary vascular remodeling and right-sided heart failure. Re-balancing this disturbed signaling using ALK5 inhibitors seems an effective therapeutic approach [22,23]. Unfortunately, the structural complexity of the TGF-β pathway (containing highly similar kinase receptors and ligands), promiscuous interactions, and factors playing numerous pleiotropic functions, causes limited target engagement, lack of specificity and adverse effects of the drugs under development. Therefore, we urge for more specific kinase inhibitors targeting TGF-β receptors to treat TGF-β related disorders.

1.2. Conventional in vitro methods to study drugs targeting TGF-β signaling

To screen for relevant drugs targeting TGF-β signaling appropriate in vitro high-throughput (HTP) methods are needed. Often used in vitro methods to measure TGF-β signaling in response to drug candidates are cross-linking based assays, transcriptional reporter systems or western blot. However, these methods share different limitations. Cross-linking approaches require radioactive isotopes and specific antibodies, often with a laborious protocol (especially in high-throughput setting) [24].

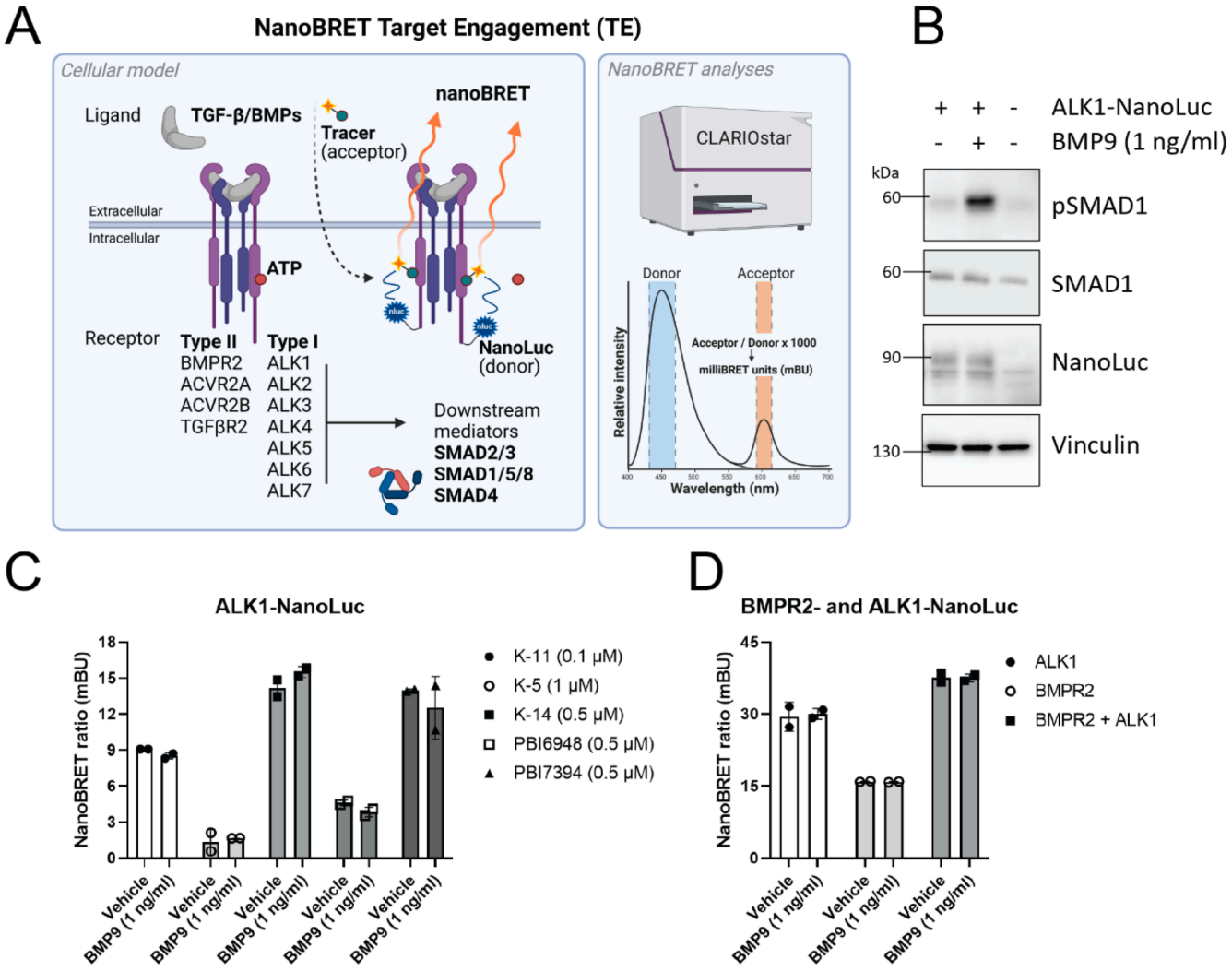

Fig. 1. TGF-β receptor activation does not increase the NanoBRET Target Engagement performance. (A) Type I and type II receptors form heterotetrameric TGF-β receptor complexes upon ligand binding. TGF-β receptor-NanoLuc fusion proteins act as nanoBRET donor whereas the membrane soluble tracer, acting as nanoBRET acceptor, can bind the TGF-β receptor kinase and this proximity enables the nanoBRET reaction. The nanoBRET ratio (milliBRET units, mBU) is calculated upon measuring the excitation values of the luminescent donor (450-80 nm) and fluorescent acceptor (590-20 nm). (B) ALK1-NanoLuc transfected Cos-1 cells were stimulated with BMP9 (1 ng/ml) for 1 h and subsequent SMAD1 phosphorylation was assessed by western blot. (C) NanoBRET TE using five different tracers (0.1 μM K-11, 1 μM K-5, 0.5 μM K-14, 0.5 μM PBI6948, and 0.5 μM PBI7394) with or without BMP9 (1 ng/ml) stimulation for 15 min prior to nanoBRET measurement on ALK1-NanoLuc transfected Cos-1 cells. Duplicates were used per condition. (D) Cos-1 cells were transfected with ALK1-NanoLuc, BMPR2-NanoLuc, or both ALK1- and BMPR2-NanoLuc and treated with a combination of K-11 (0.1 μM) and PBI7394 (0.15 μM). Subsequently, the cells were treated with and without BMP9 (1 ng/ml) for 15 min whereafter nanoBRET was measured. Duplicates were used per condition.

Transcriptional reporters, like the TGF-β responsive CAGA- and BMP responsive BRE-luciferase assays, utilize a protocol that is easier to follow, but are not receptor specific. Moreover, these assays often involve cell lysis thus only allowing end-point analysis [25,26]. The conventional western blot is not TGF-β receptor specific, it also uses protein lysates and is a low-throughput system, making it is unsuitable for kinetic high-throughput (HTP) readouts. Therefore, none of these conventional methods to measure TGF-β signaling seem good candidates for HTP screenings targeting TGF-β signaling. To study receptor-specific activity, other conventional approaches include in vitro kinase assays, surface plasmon resonance assays and (cellular) protein arrays [27,28]. The first two assays involve the purified recombinant kinase domain or full protein and are therefore easy to scale-up. However, in vitro kinase assays use high levels of ATP substrate, hence lacking a physiological environment. Surface plasmon resonance assays can be designed to mimic some physiological aspects, like a membranous substrate, but still does not resemble the full cellular complexity [27]. Alternatives to these methods, harboring the intracellular environment, are the cellular protein arrays. Some of these have limited throughput (conventional western blots) while others are more scale-able (sandwich-ELISAs or reverse protein arrays/dot blots). These assays generally use protein lysates and antibodies to detect phosphorylation sites of the protein of interest [29]. Antibody specificity is a major limiting factor, particularly when these must be raised against many different protein phosphorylation sites. In the context of TGF-β signaling, the phosphorylation status of downstream SMADs is the standard readout for pathway activation. Omics approaches (e.g. phospho-proteomics) will overcome these challenges but brings its own limitations such as costs, scale-ability, reproducibility and it also complicates the analysis pipeline. Furthermore, the need of protein lysates is not compatible with live cell kinetic responses, highly important in cellular physiology and pharmacokinetics studies. In summary, the main restraints of conventional protocols are related with: I) the lack of physiological conditions (e.g. by high ATP levels, isolated recombinant protein (domains), and in vitro setting), II) no live cell kinetic readout, and no cellular environment to III) normalize for compound membrane diffusion and/or IV) compound stability in complex intracellular settings. In screenings aiming to identify TGF-β signaling modulators, overcoming these drawbacks can facilitate the (pre-)clinical translation of potential therapeutic hits. Therefore, there is an urgent need for a method that mimics cellular complexity, is functionally relevant, and can be measured in high-throughput to screen for drug candidates targeting specific TGF-β receptors.

1.3. NanoBRET-based TGF-β receptor specific Target Engagement

To be able to address these urgent needs, in this study, a live cell Bioluminescence Resonance Energy Transfer (BRET) Target Engagement (TE) assay [30] has been optimized, adjusted and improved. This assay is applicable to a variety of TGF-β receptors, including commercial, non-commercial and newly designed constructs. In addition, the use of this system in disease relevant settings is shown. This approach

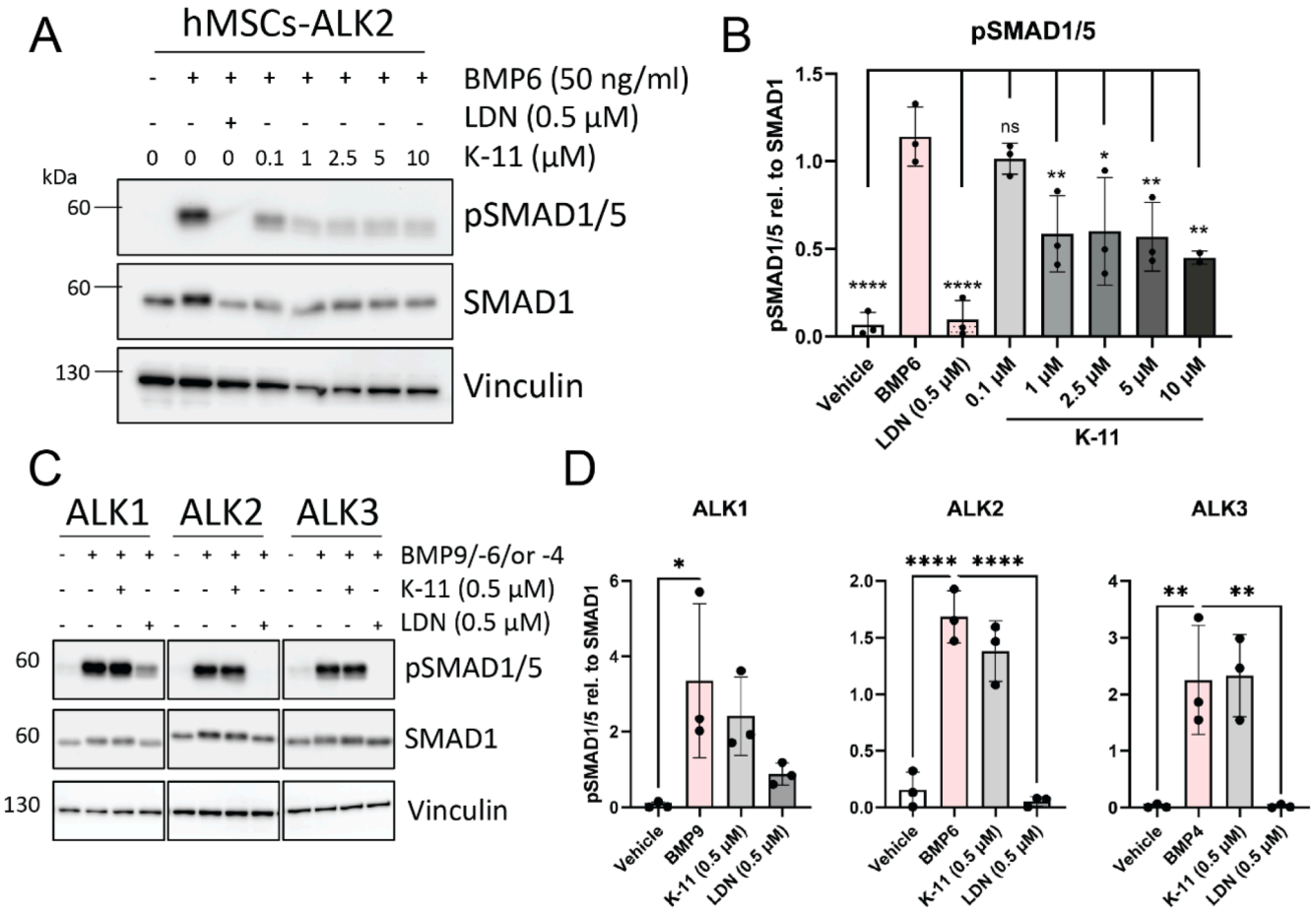

Fig. 2. The K-11 tracer can inhibit downstream TGF-β signaling, but not at the working concentration of the nanoBRET TE assay. (A) WB showing SMAD1/5 phosphorylation of ALK2-Nanoluc expressing hMSCs pre-treated with titrating concentrations of the K-11 tracer (0.1 – 10 µM) before BMP6 (50 ng/ml) stimulation. (B) Quantification of the experiment in (A) in triplicates. (C) ALK1, ALK2, or ALK3-Nanoluc expressing hMSCs were pre-treated with 0.5 µM of K-11 before being stimulated with BMP9 (1 ng/ml), BMP6 (50 ng/ml) or BMP4 (50 ng/ml), respectively. (D) Quantification of the experiment in (C) in triplicates. Significance was tested by one-way ANOVA with Dunnett's post-hoc test; ****$p<0.0001$, **$p<0.01$, *$p<0.05$.

utilizes a NanoLuc [31] luciferase BRET (NanoBRET) donor and a fluorescent tracer as BRET acceptor. The TGF-β receptor under investigation is cloned into a C-terminus Nanoluciferase (NanoLuc) expression vector, and overexpressed in cells. Upon addition of the NanoLuc substrate, this enzyme performs as BRET donor. A membrane permeable tracer with high binding affinity to the receptor kinase domain is used as BRET acceptor. Target engagement of the compound of interest can be quantified through test compound competition with the tracer molecule (Fig. 2A). Here, a comprehensive TGF-β receptor specific toolkit (Table 2) is described, with an optimized protocol to be utilized as a TGF-β receptor specific kinase inhibitor HTP screening method.

2. Methods

2.1. Cell culture

Cos-1, HEK293t and 2H11 cells were cultured in DMEM (Gibco, cat. 11965092, Thermo Fisher Scientific, Waltham, Massachusetts, USA) supplemented with 10% Fetal Bovine Serum (FBS) (Biowest, cat. S1810-500, Bradenton, Florida, USA) and 100 U/mL Pen/Strep. Additionally, the 2H11 cells were cultured on 0.1% gelatin coated plates. Bone marrow-derived human mesenchymal stem cells (hMSCs) were cultured in Alpha MEM (Gibco, cat. 32561094) supplemented with 1 ng/ml bFGF (Sigma, cat. F0291, St. Louis, Missouri, USA), 10% FBS and Pen/Strep. All cells were cultured in a CO_2 controlled 37 °C incubator. Cell passaging was performed using standard EDTA/Trypsin incubation.

2.2. Construct cloning and mutagenesis

TGF-β receptor-NanoLuc constructs (pF-32Kp backbone) were purchased from Promega (Madison, Wisconsin, USA) (ALK1-NanoLuc (NV2391), ALK2-NanoLuc (NV2341), $ALK2^{R206H}$-NanoLuc (NV2381), ALK3-NanoLuc (NV2471), and ALK4-NanoLuc (NV1021)) or acquired through collaboration with Promega R&D (ALK5-NanoLuc, TGFβR2-NanoLuc, ACVR2A-NanoLuc, ACVR2B-NanoLuc, and BMPR2-NanoLuc). The TGF-β receptor-NanoLuc inserts were subcloned into a lentiviral PLV-IRES-PURO vector. First, the restriction sites PstI, AsiSI, SalI and XbaI were PCR-amplified flanking an eGFP coding sequence and subcloned in the vector using PstI and XbaI restriction sites. Secondly, the eGFP was exchanged by the TGF-β Receptor-NanoLuc inserts via AsiSI and SalI restriction (all restriction enzymes from Thermo Fisher Scientific). Directed mutagenesis was performed using the Phusion site-directed mutagenesis kit (Thermo Fisher Scientific, cat. F541) following manufacturer's protocol. The *BMPR2* c.1454A>G mutation was introduced in the PLV-IRES-PURO_BMPR2-NanoLuc plasmid using the 5′-phosphorylated forward 5′-AAGACTGTTGGGGCCAGGATGCA-GAG-3′ and reverse 5′-CGATTGTCTCCTTGAGTGACCTCACT-3′ primers set (custom from IDT, Leuven, Belgium).

2.3. Transfections and transductions

Cos-1 cells were plated at 50% confluency in 6-wells plates the day before transfection for proper adhesion. At the end of the next day, 4 μg TGF-β receptor-NanoLuc plasmids in 250 μL DMEM and 8 μL PEI (1 mg/ml) in 250 μL DMEM were carefully mixed and incubated at room-temperature for 30 min. Cos-1 cells were refreshed to 1 mL of DMEM with 10% FBS, whereafter the lipid-DNA solution was added dropwise and incubated overnight. The next morning, the transfection medium was substituted with growth medium. Minimal 24 h after transfection, the cells were used for downstream experiments.

Adherent HEK293t cells at 50% confluency on a 15 cm^2 culture plate were transfected with 3rd generation lentiviral helper plasmids (7.5 μg pMD2g, 11.4 μg pMDLg/pRRE, 5.4 μg pRSV/REV) and the TGF-β receptor-NanoLuc encoding PLV transfer vector (13.7 μg) with 114 μL PEI (1 mg/ml) in DMEM. The medium containing the lentiviral particles was isolated 2 days after transfection and used for subsequent transduction experiments.

To generate stable TGF-β receptor-NanoLuc cell lines, Cos-1 or hMSC cells were transduced with medium containing the lentiviral particles encoding the TGF-β receptor-NanoLuc plasmid of interest. Subsequently, the transduced cells were selected by 1 μg/ml puromycin (Invivogen, cat. ant-pr-1, San Diego, California, USA) incubation for two days. These stable cell lines were used up to 20 passages without any decrease in NanoLuc-tagged receptor expression levels.

2.4. Western blot

For stimulation experiments, cells were pre-treated for 30 min with a test compound (LDN-193189, K-11 tracer or DMSO control) before stimulation with BMP9, BMP6 or BMP4 (All from R&D, cat. 3209-BP-010, 507-BP-020, 314-BP-010, respectively) for 45 min. Cell lysates were acquired upon 30-minute incubation on ice with RIPA buffer supplemented with 1X Protease Inhibitors (Roche, cat. 11836145001, Basel, Switzerland) and the phosphatase inhibitors sodium fluoride (10 mM, Sigma, cat. 7681-49-4) and sodium orthovanadate (400 μM, Sigma, cat. S6508). Subsequent protein quantification was performed using the Pierce BCA protein assay (Thermo Scientific, cat. 23225) following manufacturer's protocol. Equal protein samples (10 μg) in Laemmli Sample Buffer were loaded on 10% polyacrylamide gels for subsequent SDS-PAGE. Methanol activated PVDF membranes were used for overnight wet-transfer of the protein gels. The membranes were blocked with 10% milk (Campina, Amersfoort, The Netherlands) in TBS + Tween (TBST) and incubated with the primary antibody in 5% BSA (Sigma, cat. 05479) in TBST overnight at 4 °C. The primary antibodies used were phosho-SMAD1/5 (1:1000, Cell Signaling, cat. 9516), SMAD1 (1:1000, Cell Signaling, cat. 6944), NanoLuc (1:1000, Promega, cat. N7000), Vinculin (1:1000, Sigma, cat. V9131), or GAPDH (1:1000, Merck Millipore, cat. MAB374, Burlington, Massachusetts, USA). After a thorough wash with TBST, the membranes were incubated with secondary antibody (1:10000, Anti Mouse-HRP, Promega, cat. W4021 or Anti Rabbit-HRP, Invitrogen, cat. 31458) in 10% milk-TBST for 2 h at 4 °C. Afterwards, the washed membranes were ECL activated using WesternBright (Isogen, cat. K12042D20, Utrecht, The Netherlands) and imaged using a ChemiDoc (Bio-Rad, Hercules, California, USA). Quantification of the blots was done using densitometry in ImageJ.

2.5. Luciferase reporter assays

Sub-confluent 24-wells plates with Cos-1 cells were transfected overnight with 200 ng of the BMP responsive BRE-Luciferase reporter plasmids and 200 ng of the constitutively active (ca-) ALK1, caALK2, or caALK3 constructs in a 1:2 DNA:PEI (1 mg/ml) ratio [32]. The next day, the medium was refreshed to DMEM with titrating concentrations of test compound D (Galapagos NV), LDN-193189 or DMSO vehicle. After 24 h, the cells were washed and incubated with 160 μL of luciferase lysis buffer for 30 min on ice. Luciferase activity was measured using the Luciferase Assay System (Promega, cat. E1501) at 560 nm emission following the manufacturer's protocol. The values were normalized to total protein levels measured using the Pierce BCA assay.

2.6. NanoBRET Target Engagement assays

TGF-β receptor-NanoLuc expressing cells (transient or stable expression) were seeded on TC-treated white culture plates (Sigma, cat. CLS3917 for 96-wells or PerkinElmer, cat. 6007680, Waltham, Massachusetts, USA for 384-wells). In 96-wells format, 3*10^4 cells were seeded in 75 μL per well whereas in 384-wells format 1.5*10^4 cells were plated in 30 μL medium per well (table 1). Phenol red-free Opti-MEM (Gibco, cat. 11058021) supplemented with 1% FBS was used as seeding medium to minimize light contamination by phenol red. In the case of stimulation experiments, cells were seeded on growth medium and starved overnight by Opti-MEM without FBS. The next day, the

Table 1
Specific volumes used to perform the TGF-β Receptor-NanoLuc NanoBRET TE assays. The 96-wells and 384-wells format NanoBRET TE assay require different amounts of cells, seeding volume, tracer volume, compound/ligand volume and Nano-Glo + Inhibitor volume.

Amounts needed for nanoBRET TE	96-wells	384-wells
Cells	3*10^4	1,5*10^4
Seeding volume	75 μL	30 μL
Tracer volume (8X)	12.5 μL	5 μL
Compound/ligand volume (8X)	12.5 μL	5 μL
Nano-Glo + Inhibitor volume (3X)	33 μL	20 μL

tracer (K-11 (Promega, cat. N2652), K-5 (cat. N2482), K-14 (via Promega R&D), PBI6949 (via Promega R&D) or PBI7394 (via Promega R&D)) was added by spiking the wells with 12.5 (96-wells) or 5 μL (384-wells) of 8X concentrated tracer in Opti-MEM (from 100X tracer in tracer dilution buffer (Promega)) (Table 1). DMSO was used as vehicle control. All of these tracers were synthesized by Promega as described previously [33]. Unless otherwise stated, the tracer working concentration is depicted in Table 2. In the case of compound nanoBRET TE studies, 12.5 or 5 μL of 8X concentrated test compounds (LDN-193189, Staurosporine, compound A, B, C, D, or DMSO vehicle) were added right after tracer addition and incubated for 2 h at 37 °C. The test compounds A-D were supplied by Galapagos NV. For experiments requiring ligand stimulation, BMP9 (R&D systems, cat. 3209-BP-010/CF, Minneapolis, Minnesota, USA), BMP6 (R&D, cat. 507-BP-020/CF), or Activin A (R&D, cat. 338-AC-010/CF) ligands were spiked using 12.5 μL (96-wells) or 5 μL (384-wells) of an 8X concentrated solution in Opti-MEM. The intracellular NanoLuc activity was induced upon incubation with 3X Nano-Glo TE Substrate and Extracellular NanoLuc Inhibitor (Promega, cat. N2160) in Opti-MEM. Within 15 min after substrate addition, the plates were measured with the ClarioSTAR (BMG Labtech, Ortenberg, Germany) plate reader. The donor and acceptor excitation were measured per well using 450-80 nm and 590-20 nm filters (BMG Labtech), respectively. The interval time was set to 1s and the gain to 2500 per optic filter. The nanoBRET ratio in milliBRET units (mBU) was calculated following Eq. (1). All values were subtracted by the vehicle (no tracer) control for background correction.

Table 2
NanoBRET TE toolkit consisting of both commercially and non-commercially available TGF-β receptors and tracers. Nearly all constructs are expressed in CMV-driven pF-32Kp and PLV-IRES vectors, for either transient or stable setup. This toolkit includes the corresponding tracers, for which the manufacturer's recommended concentration (EC_{50} from transient expression in HEK293 cells) is noted. *Note that part of this toolkit is not commercially available, acquired in collaboration with Promega's R&D department or custom by ourselves.

NanoBRET toolkit	Transient Receptor-NanoLuc (pF-32Kp backbone)	Mutants	Stable Lentiviral Receptor-NanoLuc (PLV-IRES backbone)	Tracers	Tracer concentration (μM)
BMP signaling	ALK1		*Yes**	K-11	0.31
	ALK2	ALK2 p. R206H (FOP)	*Yes**	K-11	0.16
	ALK3		*Yes**	K-11	0.63
TGFβ signaling Type II	ALK4		*Yes**	K-5	2
	*ALK5**		No	*K-14**	0.5
	*TGFβR2**		*Yes**	K-11	0.32
	*ACVR2A**		*Yes**	*PBI6949**	1
	*ACVR2B**		*Yes**	*PBI6949**	1
	*BMPR2**	*BMPR2 p. D485G (PAH)**	*Yes**	*PBI7394**	0.5

$$\frac{Acceptor\ (590-20nm)}{Donor\ (450-80nm)} * 1000 \quad (1)$$

The half maximal effective concentrations (EC_{50}) and dose-response slope fitness were calculated by non-linear regression analysis of the nanoBRET measures (GraphPad Prism 10). The measures of the dose response curve experiments were normalized to vehicle (no compound) control prior to nonlinear regression analysis. The 95% confidence bands together with the SD of the data points are shown to indicate the error of the dose response curves. The fitness of the regression model was quantified using the R squared (R^2).

3. Results and discussion

Recently we have utilized nanoBRET Target Engagement (TE) to investigate potential off-target effects of a newly identified compound on various TGF-β receptors using commercially and non-commercially available receptor-NanoLuc constructs (Table 2) [34]. In that study, we used the standard manufacturer's protocol. In short, Cos-1 cells were transfected with the indicated TGF-β receptor-NanoLuc constructs and incubated for 2 h with the test compounds and the recommended concentrations of tracer (Table 2). As anticipated, the positive control kinase inhibitors (LDN-193189 [35] for ALK1/2/3, SB431542 [36] for ALK4/5, and ML347 for BMPR2) significantly inhibited the NanoBRET ratio. However, we believe that this method can be further refined. Therefore, in this study, we aimed to optimize the method to maximize the inhibitory window of TGF-β receptor specific nanoBRET Target Engagement.

3.1. *TGF-β receptor activation does not influence the nanoBRET Target Engagement capacity*

In order to optimize and enhance the nanoBRET TE assay, we hypothesized that stimulation with exogenous recombinant TGF-β ligands may induce the formation of receptor complexes including the Nanoluc-tagged receptor, thereby mediating its activation. It has been reported that ligand-induced complex formation induces a conformational change in the type I receptor which engages the kinase domain [37]. To test whether nanoBRET Target Engagement can resemble these initial steps within the sequence of activation of TGF-β family signaling, ALK1-NanoLuc expressing Cos-1 cells were preincubated with the ALK1 high-affinity ligand BMP9. Because the nanoBRET TE readout is a surrogate for the activation of the TGF-β receptor kinase activation, prior to SMAD phosphorylation, we decided to measure NanoBRET activity within 15 min after BMP9 stimulation, instead of 45 min when the peak of SMAD phosphorylation is evaluated by WB. As expected, incubation with recombinant BMP9 (1 ng/mL) efficiently induced the phosphorylation of the downstream effector SMAD1 (Fig. 1B). Despite this clear effect of BMP9, no increase in nanoBRET capacity was observed in the TE assay (Fig. 1C). Next, the response to BMP9 in the presence of sub-optimal tracer molecules was studied (Fig. 1C) to test whether a different type of tracer might be able to discriminate between a closed and open (in the presence of BMP9) conformation of the receptor. However, no differences were observed among different tracers. To test the hypothesis that the presence of a given tracer may inhibit kinase activation and therefore block TE, the K-11 tracer was preincubated at increasing concentrations prior to ALK2-NanoLuc activation. As shown in Fig. 2A-B, only very high doses of the tracer partially inhibited TGF-β signaling. No effect was observed on ALK1, -2, or -3-induced SMAD phosphorylation using tracer concentrations within the range of the TE assay working concentration (Fig. 2C-D).

Finally, given that SMAD phosphorylation occurs upon the formation of a type I and type II receptor complex, cells overexpressing BMPR2- and ALK1-NanoLuc were stimulated, followed by supplying the cells with a combinatory tracer mix (0.1 μM K-11 with 0.15 μM PBI7394). A

slight increase in the NanoBRET ratio was observed when combining tracers, however, this failed to result in an increased nanoBRET readout upon BMP9 stimulation (Fig. 1D). Given these results, the NanoBRET TE kinase assays applied to TGF-β receptors cannot discriminate between an active or inactive receptor, likely because small tracer molecules are always accessible to the receptor kinase domain, irrespective of the receptor's conformation. Designing larger ATP-like tracers might enable the detection of active TGF-β receptors using nanoBRET TE.

3.2. Stable expression of TGF-β receptor-NanoLuc constructs in human MSCs enhances nanoBRET Target Engagement performance

Next, it was determined if lentiviral mediated stable expression of the Nanoluc-tagged receptors may improve the nanoBRET ratio. No major difference in expression level was found between the two different overexpression vectors (both driven by a CMV promoter) when transfecting equal amounts of plasmid (Fig. 3A). Interestingly, the nanoBRET TE performance was increased in the stable ALK1, ALK2 or ALK3-NanoLuc expressing cell lines compared to transient expression (Fig. 3B). Noteworthy, the raw NanoLuc donor luminescence values were substantially lower in stable expressed lines compared to the transient overexpressing cells (Fig. 3E). This suggests that high TGF-β receptor-NanoLuc donor activity may hamper nanoBRET TE output, perhaps due to local tracer saturation or concentration gradients. This could not be effectively corrected with Nanoluc normalization (by acceptor-to-donor ratio calculation) and no tracer control subtraction to exclude the background noise (Fig. 3B and C). Therefore, a careful titration of the Nanoluc-expressing constructs, or the use of inducible stable expression vectors is advisable. Interestingly, further increase in the nanoBRET ratio was observed when stable overexpression of TGF-β receptor-NanoLuc constructs was performed in a different cell-line (human Mesenchymal Stem Cells; hMSCs) (Fig. 3D). This shows that (intra-)cellular complexity influences TGF-β receptor TE, perhaps due to the presence of tracer/receptor competing factors, differences in membrane surface or (extra-)cellular matrix.

3.3. Tracer titration is important to increase the performance of nanoBRET Target Engagement

Further, ALK2-NanoLuc TE was optimized because of its high nanoBRET efficiency (Fig. 3D). First, a dose dependent experiment using the commercially available K-11 tracer was performed, resulting in an EC_{50} calculation of 0.09 μM (Fig. 4A). Noteworthy, this concentration is lower than the one recommended in the manufacturer's instructions

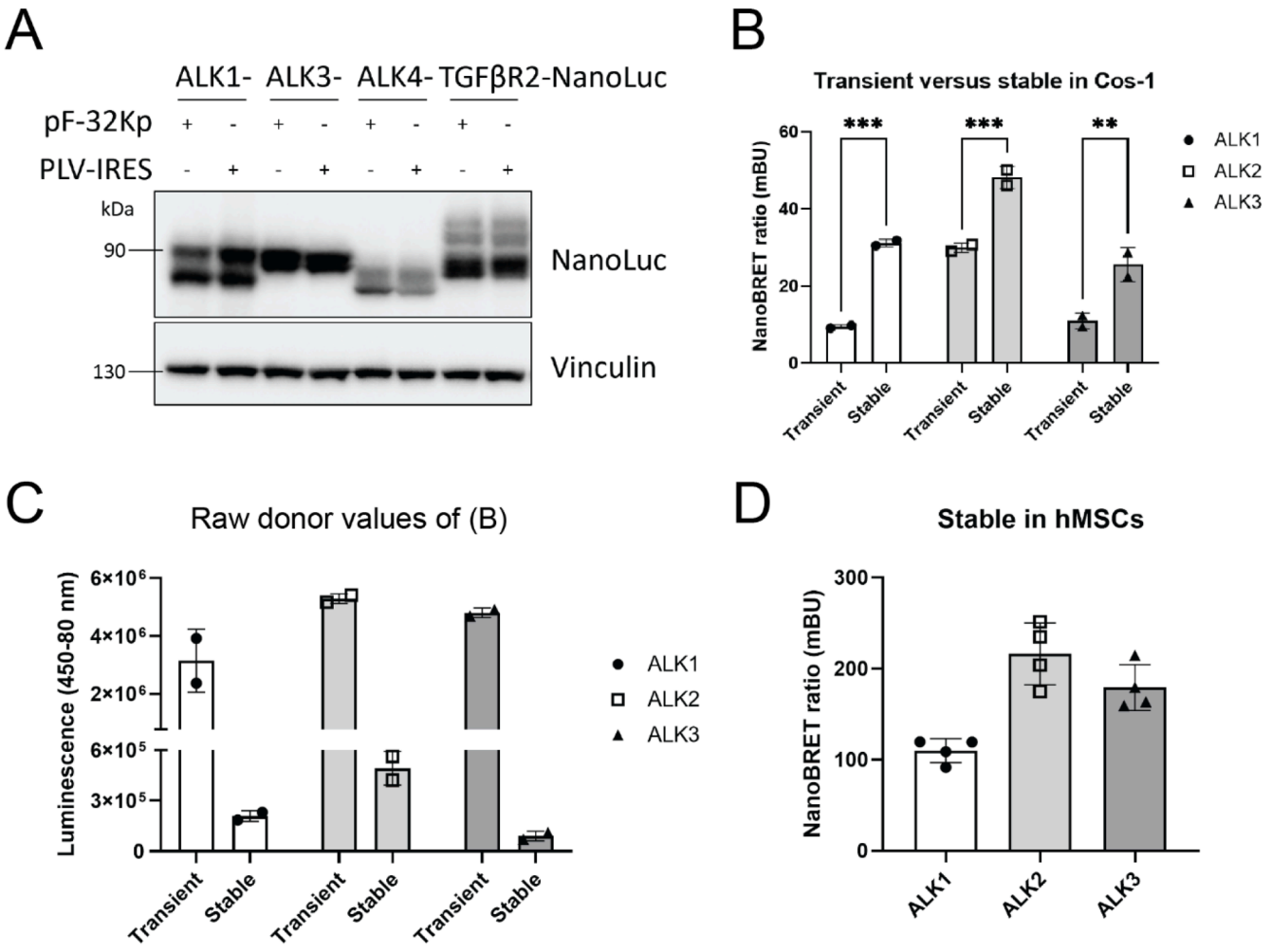

Fig. 3. Stable expression of TGF-β receptor-NanoLuc enhances nanoBRET Target Engagement performance. (A) ALK1-, ALK3-, ALK4-, and TGFβR2-NanoLuc constructs in the pF-32Kp and PLV-IRES vectors were transfected in Cos-1 cells and assessed by western blot. (B) NanoBRET TE assays of ALK1-, ALK2- and ALK3-NanoLuc in transiently and stably overexpressing Cos-1 cells. Duplicates were used per condition. (C) Raw donor values of the TGF-β receptor-NanoLuc expression levels of the assays shown in (B). (D) NanoBRET TE assays of human mesenchymal stem cells (hMSCs) stably overexpressing ALK1-, ALK2-, and ALK3-NanoLuc. Quadruplicates were used per condition. Tracer concentrations are depicted in Table 2. Statistics by one-way ANOVA with Šídák's post-hoc test; *** $p<0.001$, ** $p<0.01$.

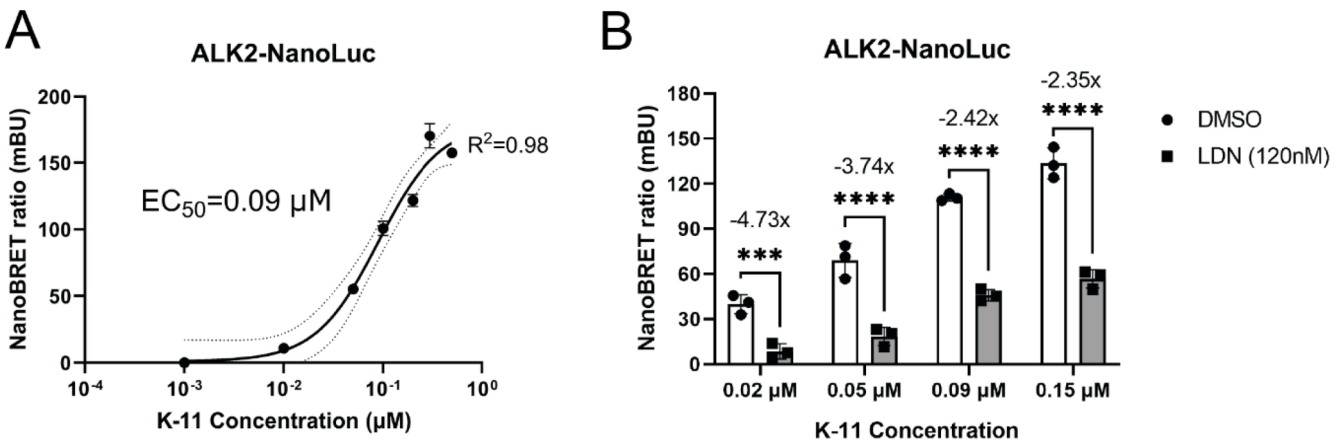

Fig. 4. Reducing the tracer concentration enhances the inhibitory window of TGF-β receptor nanoBRET Target Engagement assays. (A) Titration curve of K-11 on ALK2-NanoLuc expressing hMSCs with subsequent nanoBRET TE and EC_{50} calculations. The dotted lines indicate the 95% confidence bands. The standard deviations of some values are too low to be properly annotated. Duplicates were used per concentration. The slope fitting and EC_{50} calculation was done using non-linear regression analysis (least squares method with variable slope) in GraphPad Prism 10. (B) Reducing the tracer concentrations increases the inhibitory effect of LDN-193189 (120 nM) in hMSCs expressing ALK2-NanoLuc upon nanoBRET TE. Triplicates were used per condition. The fold reduction is calculated by dividing the mean of DMSO with the mean of LDN. Statistics by two-way ANOVA tested on the K-11 tracer concentration and the LDN treatment with Šídák's post-hoc test on the treatment condition; **** $p<0.0001$, *** $p<0.001$.

protocol (EC_{50} of 0.16 μM, Table 2), which could be explained using our stable expression setting in hMSCs instead of transient expression in HEK293 cells. After this observation, the inhibitory window of the assay was tested in combination with different tracer concentrations (Fig. 4B). For this experiment, the well-characterized BMP-receptor kinase inhibitor LDN-193189 at a low dose (120 nM) was used. Using a tracer concentration lower than the tracer EC_{50} resulted in a more potent inhibitory effect of LDN-193189 (Fig. 4B; from 2.42 times to 4.73 times ALK2 nanoBRET inhibition). Unlike in the original setting, the current optimization allowed us to obtain inhibitory levels for LDN-193189 that resemble the kinase inhibition pattern observed via SMAD phosphorylation or transcriptional reporter assays more accurately. This suggests that optimizing the optimal tracer concentration for the cell type used and generating a stable cell line expressing the TGF-β receptor-NanoLuc of interest is highly recommended.

3.4. NanoBRET Target Engagement is a fast and functional assay for pharmacological testing and high-throughput screening of kinase inhibitors targeting specific TGF-β receptors

In order to validate if nanoBRET Target Engagement is a suitable platform for drug discovery in the search for TGF-β receptor-specific kinase inhibitors, the activity of LDN-193189 (LDN) was compared with the non-selective kinase inhibitor Staurosporine. In biochemical assays, Staurosporine has a Kd of 470 nM and 3700 nM for ALK2 and ALK3, respectively, with no reported activity on ALK1 [38]. Unlike LDN, Staurosporine was unable to inhibit ALK1/2/3 target engagement at the concentrations tested (Supplementary Figure 1), suggesting that this system can identify molecules binding to the targeted receptor with enhanced affinity. Next, this method was applied to study four different investigational test compounds (compounds A-D, provided through the R&D program from Galapagos NV) using dose-response experiments on stable ALK2-NanoLuc expressing Cos-1 cells (Fig. 5A). Out of the four molecules tested, compound D (EC_{50} of 0.15 μM) is the most potent inhibitor of ALK2 kinase activity (Fig. 5A and 5C). To reassess the results obtained using NanoBRET TE with another method in living cells, the well characterized 2H11 murine endothelial cell line was used. In this cell line, the BMP6 ligand mainly activates ALK2 signaling [39]. Therefore, BMP6-induced ALK2-downstream SMAD1 phosphorylation by western blotting was used to confirm the results obtained with nanoBRET ALK2 TE (Fig. 5A). As observed in Fig. 5B, compound A was very inefficient in preventing SMAD1 activation, compounds B and C showed an intermediate activity while compound D was extremely potent with an almost complete inhibition at 0.082 μM.

Drug specificity testing, by utilizing NanoBRET TE with ALK1, ALK2 and ALK3-NanoLuc (Fig. 5C), showed that in addition to ALK2 compound D also inhibited ALK1 TE (EC_{50} of 0.34 μM), while ALK3 TE was only inhibited at high concentrations (EC_{50} of 19.77 μM) (ALK2->ALK1>>ALK3). To assess if these EC_{50} values corresponded with the often-used quantitative BMP responsive reporter line (BRE-Luc), dose-response luciferase reporter experiments were performed using compound D on constitutively active (ca-) ALK1, caALK2, and caALK3 co-expressing Cos-1 cells (Fig. 5D). Although a higher selectivity using nanoBRET TE compared to BRE-Luc was observed, the range of the EC_{50} measures was within the same order of magnitude (0.15 μM versus 0.49 μM on nanoBRET TE and BRE-Luc, respectively). Every method leads to a slightly different activity measure based on a different readout. Here, three different cell-based assays were used. Western blotting against pSMAD1/5 (Fig. 5B) shows inhibition using lower dosages of compound D compared to our BRE-Luc readout (Fig. 5D), whereas nanoBRET TE gives a selective measure for receptor inhibition. By using 384-wells plates, data corresponding to NanoBRET TE experiments (Fig. 5A and C) was collected within 3 days, in contrast to 3 weeks required to expand the cell cultures and gather the same amount of data (not all data is shown) for western blotting, which was more labor intensive. Furthermore, ligand-induced BMP receptor activation is often promiscuous and lacks complete specificity (although BMP6-ALK2 binding affinity is high). Due to the competitive origin of the nanoBRET TE assay, a high dosage (e.g., 10 μM) of the test compounds would be recommended to acquire potential hits during a compound screen. Subsequently, one can titrate the hits and validate their potential using SMAD phosphorylation or reporter lines. In conclusion, the nanoBRET TE assay is fast, high-throughput and shows functionally relevant to use as a TGF-β receptor specific kinase inhibitor screening method.

3.5. Mutated TGF-β receptor-NanoLuc constructs enable disease relevant studies by utilizing nanoBRET Target Engagement

To further tailor this method for patient-specific purposes, disease relevant TGF-β receptor-NanoLuc mutants were generated in lentiviral constructs for a stable expression setup. The ALK2 c.617G>A (p.R206H) construct is commercially available for transient expression. In addition, the BMPR2 c.1454A>G (p.D485G) mutant construct was generated via site-directed mutagenesis (Fig. 6B), resembling an FOP ALK2 mutant

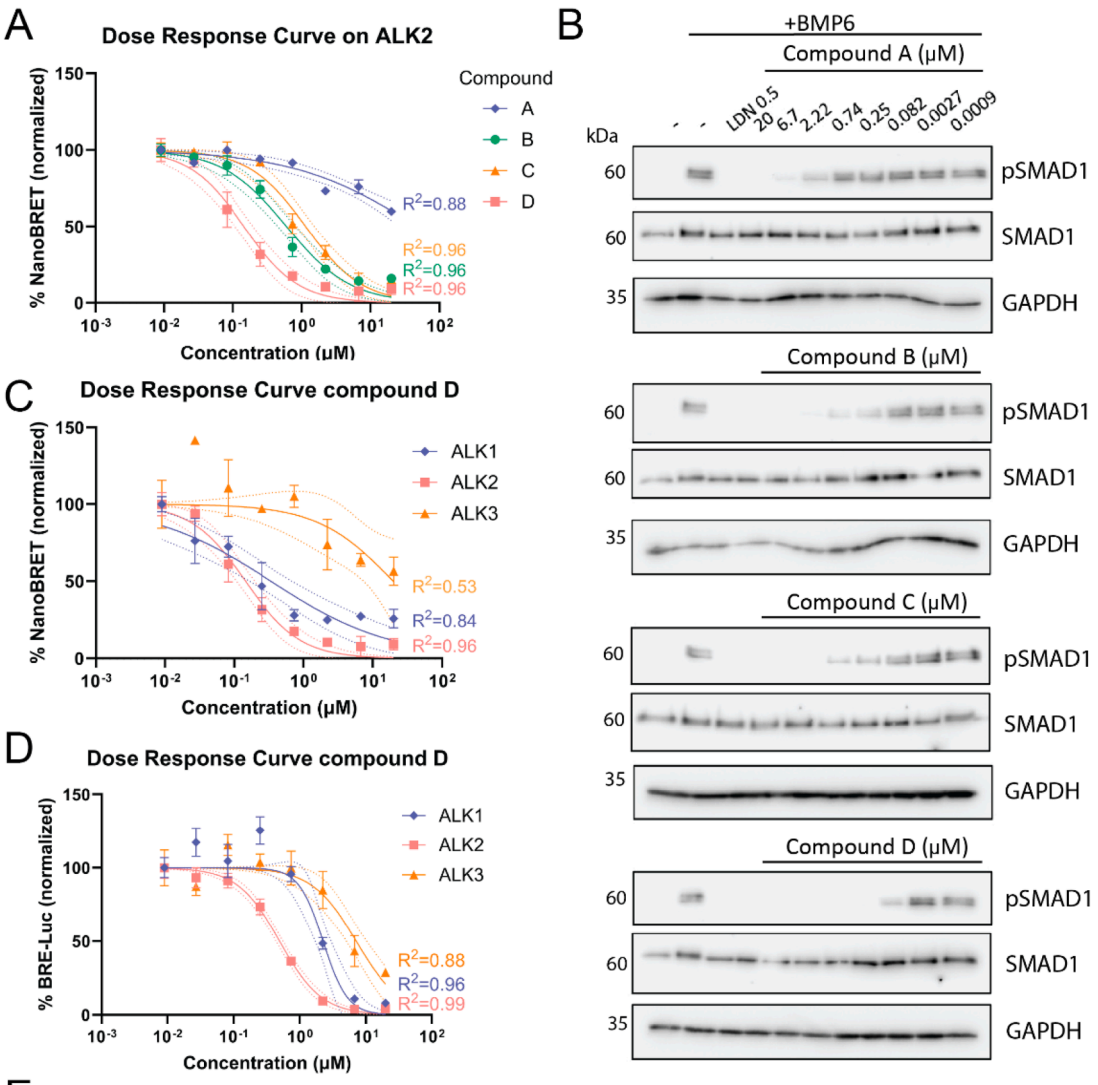

E

Compound	Target	$EC_{50\_nanoBRET}$ (μM)	$EC_{50\_BRE\text{-}luc}$ (μM)
A	ALK2	-	-
B	ALK2	0.60	-
C	ALK2	1.14	-
D	ALK2	0.15	0.49
D	ALK1	0.34	2.25
D	ALK3	19.77	7.13

Fig. 5. NanoBRET Target Engagement is a fast and functional method to test TGF-β receptor kinase inhibition. (A) Dose response curve of four test compounds (compound A-D) on stable ALK2-NanoLuc expressing Cos-1 cells using NanoBRET TE. Duplicates were used per condition. (B) Immunostaining of SMAD1 phosphorylation after dosing of the four different test compounds and subsequent 1 h BMP6-induced (50 ng/ml) ALK2 activation in 2H11 cells. A high dose of LDN-193189 (0.5 μM) was used as positive control. (C) Dose response curve of compound D on stable ALK1-, ALK2-, or ALK3-NanoLuc expressing Cos-1 cells assessed by nanoBRET TE. All nanoBRET ratios were normalized to vehicle controls. The tracer K-11 concentrations were 0.31 μM for ALK1-, 0.09 μM for ALK2-, and 0.63 μM for ALK3-NanoLuc. Duplicates were used per condition. (D) Dose response curve of compound D assessed on the BMP responsive BRE-Luciferase measurements using constitutively active ALK1, ALK2 or ALK3 in Cos-1 cells. The experiment was performed in triplicates. The 95% confidence bands are depicted by the dotted lines in all the dose response curves shown in this figure. Some of the standard deviations are too low to be depicted accordingly. (E) The slope fitness and corresponding EC50 values of (A), (C) and (D) were calculated by non-linear normalized regression analysis in GraphPad Prism 10.

receptor and a BMPR2 mutation observed in Pulmonary Arterial Hypertension (PAH) patients, respectively. FOP is caused by a gain-of-function mutation harboring $ALK2^{R206H}$ responsive to Activin A [40], while this is not the case for wild-type ALK2 (Fig. 6A). PAH mutations are loss-of-function, where the D485G mutation disrupts two hydrogen bonds at the kinase domain of BMPR2 [41]. Harboring a C-terminal NanoLuc for TGFBRs, these mutated constructs are effectively expressed and remain functional, as observed by Activin A-induced SMAD1 phosphorylation in $ALK2^{R206H}$-NanoLuc expressing hMSCs (Fig. 6A and C) [40]. Although diseased SMAD1/5 signaling can be observed by western blotting, the $ALK2^{R206H}$-NanoLuc lines show a similar nanoBRET TE capacity compared to the wild-type ALK2-NanoLuc (Fig. 6D). This might be related to the previously discussed high binding efficiency of the tracer, unable to distinguish between an inactive and an engaged

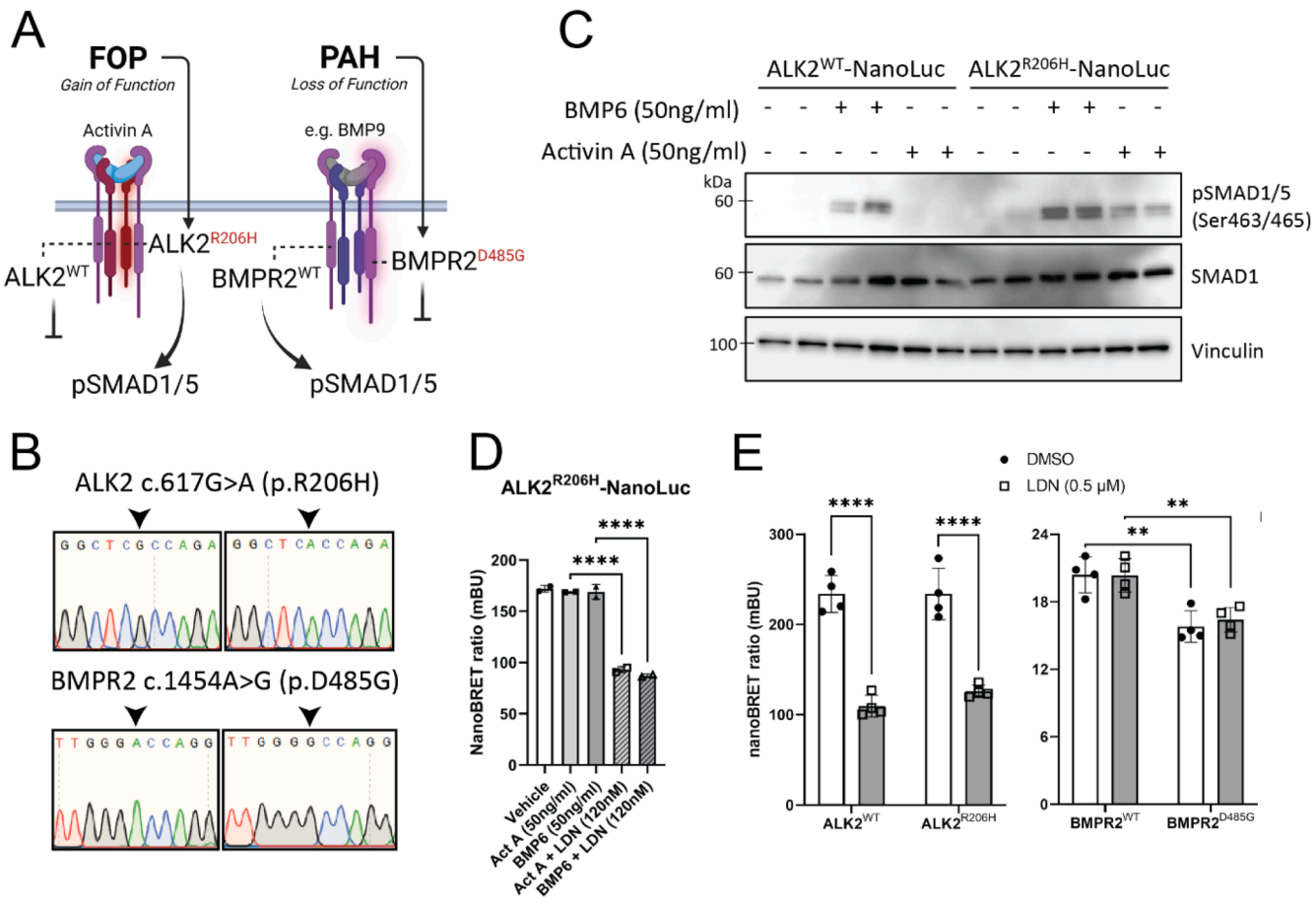

Fig. 6. Mutated TGF-β receptor-NanoLuc constructs enable disease relevant studies. (A) The gain-of-function mutation ALK2^{R206H} causes FOP and the loss-of-function BMPR2^{D485G} can result in PAH. The ALK2^{R206H} receptor is prone to Activin A activation while the BMPR2^{D485G} receptor shows reduced downstream signaling. (B) Sanger sequencing analysis of the mutation site shows the correct base substitutions in ALK2^{WT}- versus ALK2^{R206H}-NanoLuc and BMPR2^{WT}- versus BMPR2^{D485G}-NanoLuc constructs. (C) Confirmation of diseased SMAD signaling in ALK2^{R206H}-NanoLuc expressing hMSCs. Mutant lines show differential SMAD1/5 phosphorylated upon 1 h of Activin A (50 ng/ml) stimulation compared to controls, assessed by western blot. (D) ALK2^{R206H}-NanoLuc activation cannot be measured by NanoBRET TE upon Activin A (50 ng/ml) or BMP6 (50 ng/ml) stimulation. A low dose of LDN-193189 (120 nM) is able to significantly reduce the nanoBRET TE of the activated receptors. Duplicates were used per condition. (E) NanoBRET TE analyses of mutant ALK2- and BMPR2-NanoLuc constructs with their respective wild-type controls. The R206H mutation in ALK2 does not show any reduced nanoBRET output, while the D485G kinase mutation in BMPR2 reduces the tracer accessibility compared to the wild-type receptors. Quadruplicates were used per condition. Statistics by one-way (D) or two-way (E) ANOVA with Tukey's multiple comparisons test; **** $p<0.0001$, ** $p<0.01$.

TGF-β kinase receptor (Fig. 1). In line, the nanoBRET TE capacity could not be enhanced by stimulating ALK2^{WT} or ALK2^{R206H}-NanoLuc cells with exogenous ALK2 ligands (Fig. 6D). Interestingly, comparing the wild-type and the diseased BMPR2 construct revealed that the loss-of-function mutation D485G in PAH reduced the nanoBRET TE capacity, suggesting an impaired lower tracer accessibility (Fig. 6E). No difference in expression levels was observed (data not shown). In line, mutations in the cytosolic domain of BMPR2 have been shown to disrupt structural stability [41,42]. Importantly, despite this lack of measured diseased BMPR2^{D485G} signaling in this study, this new BMPR2^{D485G}-NanoLuc TE readout may be used to screen for compounds normalizing the tracer accessibility, hence identifying promising PAH-specific therapies targeting BMPR2. Alternatively, one could try to rebalance the disturbed TGF-β signaling to screen for ALK4 inhibitors to block the aberrant Activin A signaling in PAH [43,44], a similar approach is currently investigated in clinical studies by treatment of PAH patients with ACTR2A-Fc (Sotatercept) [45]. In summary, mutated TGF-β receptor-NanoLuc expressing cells can be used to study diseased signaling and are suitable in nanoBRET TE setting to screen for disease specific kinase inhibitors or activators.

In this study, it is shown that NanoBRET Target Engagement is a promising technique to use as TGF-β receptor specific kinase inhibitor screening method in a disease relevant setting. The original protocol has been refined to enhance the TGF-β receptor nanoBRET capacity and inhibitory window by using a stable expression setup in a different cell line and reducing the tracer concentration. By testing multiple compounds on different TGF-β receptors it is demonstrated that nanoBRET TE is a fast, high-throughput and functional assay to study TGF-β receptor specific kinase inhibitors. Finally, this system can be utilized for disease-relevant studies by introducing mutations in the TGF-β receptor-NanoLuc constructs. Thus, this optimized intracellular TGF-β receptor specific nanoBRET Target Engagement assay is a functional and antibody-independent kinase assay highly promising for TGF-β receptor specific kinase compound screenings improving the lead-to-success rate due to enhanced methodology. We hope that our research sets the base for upcoming studies identifying novel TGF-β receptor kinase inhibitors or activators for the treatment of TGF-β associated disorders.

Funding

We acknowledge the support from Promega R&D. Galapagos NV provided funding for the conduct of the study and the compounds A-D. Some figures were made using Biorender.com. This research was further supported by grants Ramón y Cajal RYC2021-030866-I, PID2022-

141212OA-I00 and CNS2023-145432 from the Spanish Ministry of Science and Innovation (to GSD). GSD is also sponsored by La Marató de TV3 (202038-30), the BHF-DZHK-DHF, 2022/23 award PROMETHEUS (02-001-2022-0123), the Foundation Eugenio Rodriguez Pascual (FERP-2023-058) and the Foundation "Por dos pulgares de nada". MW and MJG are sponsored by the Netherlands Cardiovascular Research Initiative (the Dutch Heart Foundation, Dutch Federation of University Medical Centers, the Netherlands Organization for Health Research and Development, and the Royal Netherlands Academy of Sciences), PHAEDRA-IMPACT (DCVA) and DOLPHIN-GENESIS (CVON). Finally, we thank the Scientific Research Network by the Research Foundation–Flanders (WOG W0014200N) and An Zwijsen.

CRediT authorship contribution statement

Marius Wits: Investigation, Formal analysis, Conceptualization. **Nicole Haarmans:** Formal analysis, Data curation. **Gonzalo Sanchez-Duffhues:** Writing – review & editing, Supervision, Resources, Funding acquisition, Conceptualization. **Marie-José Goumans:** Writing – review & editing, Resources, Funding acquisition.

Declaration of competing interest

The authors declare the following financial interests/personal relationships which may be considered as potential competing interests: Gonzalo Sanchez Duffhues reports financial support was provided by Spain Ministry of Science and Innovation. Gonzalo Sanchez Duffhues reports financial support was provided by Por Dos Pulgares de Nada. Gonzalo Sanchez Duffhues reports financial support was provided by Eugenio Rodríguez Pascual Foundation. Gonzalo Sanchez Duffhues reports financial support was provided by Fundació La Marató de TV3. Gonzalo Sanchez Duffhues reports financial support was provided by Netherlands Heart Foundation. Marius Wits reports financial support was provided by Dutch CardioVascular Alliance. Gonzalo Sanchez Duffhues reports financial support was provided by Galapagos NV. Gonzalo Sanchez Duffhues reports a relationship with Promega Benelux BV that includes: non-financial support. If there are other authors, they declare that they have no known competing financial interests or personal relationships that could have appeared to influence the work reported in this paper.

Supplementary materials

Supplementary material associated with this article can be found, in the online version, at doi:10.1016/j.slasd.2024.100196.

References

[1] Morikawa M, Derynck R, Miyazono K. TGF- β and the TGF-β family: context-dependent roles in cell and tissue physiology. Cold Spring Harb Perspect Biol 2016; 8(5). https://doi.org/10.1101/cshperspect.a021873.
[2] Kingsley DM. The TGF-β superfamily: new members, new receptors, and new genetic tests of function in different organisms. Genes Dev 1994;8(2):133–46. https://doi.org/10.1101/gad.8.2.133.
[3] Javelaud D, Mauviel A. Mammalian transforming growth factor-βs: Smad signaling and physio-pathological roles. Int J Biochem Cell Biol 2004;36(7):1161–5. https://doi.org/10.1016/S1357-2725(03)00255-3.
[4] Sanchez-Duffhues G, Williams E, Goumans MJ, Heldin CH. ten Dijke P. Bone morphogenetic protein receptors: structure, function and targeting by selective small molecule kinase inhibitors. Bone 2020;138. https://doi.org/10.1016/j.bone.2020.115472.
[5] Heldin CH, Moustakas A. Signaling receptors for TGF-β family members. Cold Spring Harb Perspect Biol 2016;8(8):1–33. https://doi.org/10.1101/cshperspect.a022053.
[6] Derynck R. TGF-β-receptor-mediated signaling. Trends Biochem Sci 1992;1994: 168–94. https://doi.org/10.1093/oxfordhb/9780199215362.013.8.
[7] Gipson GR, Goebel EJ, Hart KN, et al. Structural perspective of BMP ligands and signaling. Bone 2020;140:115549. https://doi.org/10.1016/j.bone.2020.115549.
[8] Chang C. Agonists and antagonists of TGF-β family ligands. Cold Spring Harb Perspect Biol 2016;8(8):1–51. https://doi.org/10.1101/cshperspect.a021923.
[9] Nickel J, Ten Dijke P, Mueller TD. TGF-β family co-receptor function and signaling. Acta Biochim Biophys Sin (Shanghai) 2018;50(1):12–36. https://doi.org/10.1093/abbs/gmx126.
[10] Miyazono K, Ten Dijke P, Heldin CH. TGF-β signaling by Smad proteins. Adv Immunol 2000;75:115–57. https://doi.org/10.1016/s0065-2776(00)75003-6.
[11] Hayashi H, Abdollah S, Qiu Y, et al. The MAD-related protein Smad7 associates with the TGFβ receptor and functions as an antagonist of TGFβ signaling. Cell 1997; 89(7):1165–73. https://doi.org/10.1016/S0092-8674(00)80303-7.
[12] Hata A, Lagna G, Massagué J, Hemmati-Brivanlou A. Smad6 inhibits BMP/Smad1 signaling by specifically competing with the Smad4 tumor suppressor. Genes Dev 1998;12:186–97. www.genesdev.org.
[13] Biernacka A, Dobaczewski M, Frangogiannis NG. TGF-β signaling in fibrosis. Growth Factors 2011;29(5):196–202. https://doi.org/10.3109/08977194.2011.595714.TGF.
[14] Massagué J, Sheppard D. TGF-β signaling in health and disease. Cell 2023;186(19): 4007–37. https://doi.org/10.1016/j.cell.2023.07.036.
[15] Bierie B, Moses HL. Tumour microenvironment - TGFB: the molecular Jekyll and Hyde of cancer. Nat Rev Cancer 2006;6(7):506–20. https://doi.org/10.1038/nrc1926.
[16] Pignolo RJ, Shore EM, Kaplan FS. Fibrodysplasia ossificans progressiva: clinical and genetic aspects. Orphanet J Rare Dis 2011;6(1):80. https://doi.org/10.1186/1750-1172-6-80.
[17] Goumans MJ, ten Dijke P. TGF-β signaling in control of cardiovascular function. Cold Spring Harb Perspect Biol 2018;10(2):1–40. https://doi.org/10.1101/cshperspect.a022210.
[18] Huang CY, Chung CL, Hu TH, Chen JJ, Liu PF, Chen CL. Recent progress in TGF-β inhibitors for cancer therapy. Biomedicine and Pharmacotherapy 2021;134. https://doi.org/10.1016/j.biopha.2020.111046.
[19] Hopkins CR. Inhibitors of the bone morphogenetic protein (BMP) signaling pathway: a patent review (2008–2015). Expert Opin Ther Pat 2016;26(10): 1115–28. https://doi.org/10.1080/13543776.2016.1217330.
[20] Yu PB, Deng DY, Lai CS, et al. BMP type I receptor inhibition reduces heterotopic ossification. Nat Med 2008;14(12):1363–9. https://doi.org/10.1038/nm.1888.
[21] Davis AJ, Brooijmans N, Brubaker JD, et al. An ALK2 inhibitor, BLU-782, prevents heterotopic ossification in a mouse model of fibrodysplasia ossificans progressiva. Sci Transl Med 2024;16:eabp8334. https://www.science.org.
[22] Zaiman AL, Podowski M, Medicherla S, et al. Role of the TGF-β/Alk5 signaling pathway in monocrotaline-induced pulmonary hypertension. Am J Respir Crit Care Med 2008;177(8):896–905. https://doi.org/10.1164/rccm.200707-1083OC.
[23] Thomas M, Docx C, Holmes AM, et al. Activin-like kinase 5 (ALK5) mediates abnormal proliferation of vascular smooth muscle cells from patients with familial pulmonary arterial hypertension and is involved in the progression of experimental pulmonary arterial hypertension induced by monocrotaline. Am J Pathol 2009;174 (2):380–9. https://doi.org/10.2353/ajpath.2009.080565.
[24] Cheifetzs S, Like B, Massague J. Cellular distribution of type I and type II receptors for transforming growth factor-β. J Biol Chem 1986;261(21):9972–8.
[25] Korchynskyi O, Ten Dijke P. Identification and functional characterization of distinct critically important bone morphogenetic protein-specific response elements in the Id1 promoter. J Biol Chem 2002;277(7):4883–91. https://doi.org/10.1074/jbc.M111023200.
[26] Dennler S, Itoh S, Vivien D, Ten Dijke P, Phane Huet S, Gauthier JM. Direct binding of Smad3 and Smad4 to critical TGFβ-inducible elements in the promoter of human plasminogen activator inhibitor-type 1 gene. EMBO J 1998;17:3091–100. https://www.embopress.org.
[27] De Mol NJ, Fischer MJE. Surface plasmon resonance methods and protocols. In: Methods in molecular biology. 627; 2010. www.springer.com/series/7651.
[28] Ma H, Deacon S, Horiuchi K. The challenge of selecting protein kinase assays for lead discovery optimization. Expert Opin Drug Discov 2008;3(6):607–21. https://doi.org/10.1517/17460441.3.6.607.
[29] Martiny-Baron G, Haasen D, D'Dorazio D, Voshol J, Fabbro D. Characterization of kinase inhibitors using reverse phase protein arrays. Methods in molecular biology, 785. Humana Press Inc.; 2011. p. 79–107. https://doi.org/10.1007/978-1-61779-286-1_7.
[30] Robers MB, Dart ML, Woodroofe CC, et al. Target engagement and drug residence time can be observed in living cells with BRET. Nat Commun 2015;6. https://doi.org/10.1038/ncomms10091.
[31] England CG, Ehlerding EB, Cai W. NanoLuc: a small luciferase is brightening up the field of bioluminescence. Bioconjug Chem 2016;27(5):1175–87. https://doi.org/10.1021/acs.bioconjchem.6b00112.
[32] Sánchez-Duffhues G, Williams E, Benderitter P, et al. Development of macrocycle kinase inhibitors for ALK2 using fibrodysplasia ossificans progressiva-derived endothelial cells. JBMR Plus 2019;3(11). https://doi.org/10.1002/jbm4.10230.
[33] Vasta JD, Corona CR, Wilkinson J, et al. Quantitative, wide-spectrum kinase profiling in live cells for assessing the effect of cellular ATP on target engagement. Cell Chem Biol 2018;25(2):206–14. https://doi.org/10.1016/j.chembiol.2017.10.010. e11.
[34] Valer JA, Deber A, Wits M, et al. PI3Kα inhibition blocks osteochondroprogenitor specification and the hyper-inflammatory response to prevent heterotopic ossification. Elife 2023. https://doi.org/10.7554/eLife.91779.1. Published online.
[35] Boergermann JH, Kopf J, Yu PB, Knaus P. Dorsomorphin and LDN-193189 inhibit BMP-mediated Smad, p38 and Akt signalling in C2C12 cells. Int J Biochem Cell Biol 2010;42(11):1802–7. https://doi.org/10.1016/j.biocel.2010.07.018.
[36] Inman GJ, Nicolas FJ, Callahan JF, et al. SB-431542 is a potent and specific inhibitor of transforming growth factor-superfamily type I Activin Receptor-Like Kinase (ALK) receptors ALK4, ALK5, and ALK7. Mol Pharmacol 2002;62(1):65–74. http://molpharm.aspetjournals.org.

[37] Hinck AP, Mueller TD, Springer TA. Structural biology and evolution of the TGF-β family. Cold Spring Harb Perspect Biol 2016;8(12):1–51. https://doi.org/10.1101/cshperspect.a022103.
[38] Karaman MW, Herrgard S, Treiber DK, et al. A quantitative analysis of kinase inhibitor selectivity. Nat Biotechnol 2008;26(1):127–32. https://doi.org/10.1038/nbt1358.
[39] Sánchez-Duffhues G, García de Vinuesa A, van de Pol V, et al. Inflammation induces endothelial-to-mesenchymal transition and promotes vascular calcification through downregulation of BMPR2. J Pathol 2019;247(3):333–46. https://doi.org/10.1002/path.5193.
[40] Hino K, Ikeya M, Horigome K, et al. Neofunction of ACVR1 in fibrodysplasia ossificans progressiva. Proc Natl Acad Sci USA 2015;112(50):15438–43. https://doi.org/10.1073/pnas.1510540112.
[41] Chaikuad A, Thangaratnarajah C, von Delft F, Bullock AN. Structural consequences of BMPR2 kinase domain mutations causing pulmonary arterial hypertension. Sci Rep 2019;9(1). https://doi.org/10.1038/s41598-019-54830-7.
[42] Agnew C, Ayaz P, Kashima R, et al. Structural basis for ALK2/BMPR2 receptor complex signaling through kinase domain oligomerization. Nat Commun 2021;12(1). https://doi.org/10.1038/s41467-021-25248-5.
[43] Yndestad A, Larsen KO, Øie E, et al. Elevated levels of activin A in clinical and experimental pulmonary hypertension. J Appl Physiol 2009;106(4):1356–64. https://doi.org/10.1152/japplphysiol.90719.2008.
[44] Guignabert C, Savale L, Boucly A, et al. Serum and pulmonary expression profiles of the activin signaling system in pulmonary arterial hypertension. Circulation 2023:1–13. https://doi.org/10.1161/CIRCULATIONAHA.122.061501. Published online.
[45] Hoeper MM, Badesch DB, Ghofrani HA, et al. Phase 3 trial of sotatercept for treatment of pulmonary arterial hypertension. N Engl J Med 2023:1–13. https://doi.org/10.1056/NEJMoa2213558. Published online.